Author Manuscript

Author Manuscript

Author Manuscript

Author Manuscript

HHS Public Access

Author manuscript

Int J Dev Neurosci. Author manuscript; available in PMC 2021 December 01.

Published in final edited form as:

Int J Dev Neurosci. 2020 December ; 80(8): 717–729. doi:10.1002/jdn.10071.

Quantitative analyses of high angular resolution diffusion imaging (HARDI)-derived long association fibers in children with sensorineural hearing loss

Tadashi Shiohama[1,2], **Brianna Chew**[3], **Jacob Levman**[1,4], **Emi Takahashi**[1]

[1]Division of Newborn Medicine, Department of Medicine, Boston Children's Hospital, Harvard Medical School, 300 Longwood Avenue, Boston, MA 02115, USA

[2]Department of Pediatrics, Chiba University Hospital, Inohana 1-8-1, Chiba-shi, Chiba 2608670, Japan

[3]College of Science, Northeastern University, 360 Huntington Ave, Boston, MA 02115, USA

[4]Department of Mathematics, Statistics and Computer Science, St. Francis Xavier University, 2323 Notre Dame Ave, Antigonish, Nova Scotia B2G 2W5, Canada

Abstract

Sensorineural hearing loss (SNHL) is the most common developmental sensory disorder due to a loss of function within the inner ear or its connections to the brain. While successful intervention for auditory deprivation with hearing amplification and cochlear implants during a sensitive early developmental period can improve spoken-language outcomes, SNHL patients can suffer several cognitive dysfunctions including executive function deficits, visual cognitive impairment, and abnormal visual dominance in speaking perception even after successful intervention. To evaluate whether long association fibers are involved in the pathogenesis of impairment on the extra-auditory cognitive process in SNHL participants, we quantitatively analyzed high-angular resolution diffusion imaging (HARDI) tractography-derived fibers in participants with SNHL. After excluding cases with congenital disorders, perinatal brain damage, or premature birth, we enrolled 17 participants with SNHL aged under 10 years old. Callosal pathways (CP) and 6 types of cortico-cortical association fibers (arcuate fasciculus [AF], inferior longitudinal fasciculus [ILF], inferior fronto-occipital fasciculus [IFOF], uncinate fasciculus [UF], cingulum fasciculus

Corresponding author: Tadashi Shiohama, M.D., Ph.D., Department of Pediatrics, Chiba University Hospital, 1-8-1 Inohana, Chuo-ku, Chiba-shi, Chiba 260-8670, Japan, Tel: +81(43)226-2144, Fax: +81(43)226-2145, asuha_hare@yahoo.co.jp.

Author Contributions

T.S. was responsible for study design. J.L. assembled data. T.S., B.C., and E.T. analyzed data. T.S., J.L., and E.T. wrote/edited the manuscript.

Conflict of Interest

T.S., B.C., J. L., and E. T. declare relevant no conflicts of interest.

Ethical approval

All procedures performed in the studies involving human participants were in accordance with the ethical standards of the institutional and/or national research committee and with the 1964 Helsinki Declaration and its later amendments or comparable ethical standards.

Informed consent

For this type of study, formal consent is not required.

Data Availability Statement

The data that support the findings of this study are available from the corresponding author upon reasonable request.

Author Manuscript Author Manuscript Author Manuscript Author Manuscript

[CF], and fornix [Fx]) in both hemispheres were identified and visualized. The ILF and IFOF were partly undetected in three profound SNHL participants. Compared to age- and gender-matched neurotypical controls (NC), decreased volumes, increased lengths, and high apparent diffusion coefficient (ADC) values without difference in fractional anisotropy (FA) values were identified in multiple types of fibers in the SNHL group. The impairment of long association fibers in SNHL may partly be related to the association of cognitive dysfunction with SNHL.

Keywords

Sensorineural hearing loss; high-angular resolution diffusion imaging; long association fibers; apparent diffusion coefficient; fractional anisotropy

1. Introduction

Sensorineural hearing loss (SNHL) is the most common developmental sensory disorder due to a loss of function within the inner ear or its connections to the brain (Martines et al., 2013). SNHL in childhood is mainly caused by cochlear dysfunction due to genetic syndromes, congenital infections, and meningitis (Kral & O'Donoghue, 2010). Auditory deprivation at the fetal period affects neurocognitive functions via the decrease of auditory input or the secondary restriction of social communications (Kral et al., 2016). Even after successful intervention, children with congenital hearing loss can suffer several cognitive dysfunctions including executive function deficits (Kronenberger et al., 2014), visual cognitive impairment (Dye, 2014; Dye & Hauser, 2014; Turgeon et al., 2012), and abnormal visual dominance in speaking perception (Bergeson et al., 2010; Buckley and Tobey, 2011) as well as language delay (Tomblin et al., 2015; Yoshinaga-Itano et al., 2017).

The cochlear function and afferent auditory pathway are established from 23–26 weeks after conception (Kral et al., 2016), which precedes the sulcation of the ventral and lateral surface (Garel et al., 2003). Auditory input during the fetal period modulates human brain development (Kral and O'Donoghue, 2010; Kral et al., 2013, 2016; Berger et al., 2017). Therefore, hearing deprivation *in utero* would disturb functional maturation, delay cortical synaptogenesis, and increase subsequent synaptic elimination (Kral and O'Donoghue, 2010; Kral et al., 2013, 2016). A pathohistological study showed that congenital SNHL affects the deep layer of the primary and secondary auditory cortex in human patients and animal models (Berger et al., 2017). In addition, the primary auditory area has functional connections with the primary visual area in humans (Watanabe et al., 2013; Vetter et al., 2014; Petro et al., 2017; Raij et al., 2010). These reports may explain why broad cognitive dysfunctions are observed in SNHL patients.

To identify the structural changes in auditory and cognitive dysfunctions in children and adults with SNHL, several neuroimaging studies have been carried out, and have shown that decreased thickness in the left lateral occipital cortex (Shiohama et al., 2019a), can be observed in SNHL children. On the other hand, several studies have reported that the auditory area in SNHL patients was innervated by other sensory systems (Lomber et al., 2010; Sadato et al., 2005). Interestingly, prior structural MRI studies have independently

Author Manuscript Author Manuscript Author Manuscript Author Manuscript

observed that volumes of gray matter in auditory areas are preserved in SNHL (Shiohama et al., 2019a; Shibata et al., 2007; Hribar et al., 2014; Li et al., 2012).

In contrast to cortical morphometry studies using T1-weighted images, there are only a few studies concerning diffusion MRI in children with SNHL (Chang et al., 2012; Wu et al., 2016; Jiang et al., 2019; Wang H et al., 2019; Wang S et al., 2019; Park et al., 2018). These studies mainly focus on fractional anisotropy (FA) values in auditory pathways (lemniscus lateralis, inferior colliculus, medial geniculate bodies, and auditory radiations) and speech composition centers (e.g. Broca's gyrus, and Heschl's gyrus), and there is no quantitative study of tractography-based long association fibers to our best knowledge. Hence, whether and how long association fibers are affected in congenital SNHL still remains unclear. The long association fibers play a key role in intellectual abilities such as speech and language processing (Friederici, 2015), arithmetic processing (McCaskey, et al., 2020), motor imagery processing (Oostra et al., 2016), and cognitive functions (Filley & Fields, 2016). The aim of this study is to investigate the pathogenesis of non-verbal cognitive dysfunction in SNHL by quantitatively analyzing long association fibers in children with SNHL.

2. Patients and Methods

2.1. Patients

We reviewed electronic medical records from June 1st, 2008 to February 24th, 2016, with approval by the Institutional Review Board at Boston Children Hospital, and identified participants aged under 10 years old (YO) with SNHL according to audiometric tests and otolaryngologic examinations as in our previous study (Shiohama et al., 2019a). The degree of SNHL was determined as mild to moderate (M-M, 26–55 dB HL) and moderately severe to profound (M-P, over 56 dB HL) according to the average of hearing thresholds at 500, 1000, and 2000 Hz for pure tone tests of their better ear or sound-field visual reinforcement audiometry tests (Yoshinaga-Itano et al., 2017). We excluded patients with congenital disorders (e.g. Down syndrome, CHARGE syndrome, and other chromosomal abnormalities), perinatal brain damage (hypoxic ischemic encephalopathy and infarction), and premature birth (<37 weeks gestation). The gender- and age-matched neurotypical controls (NC) were selected from our in-house database composed of electronic records of healthy participants without neurological disorders, neuropsychological disorders or epilepsy (Levman et al., 2017).

2.2. Acquisition and processing for diffusion MRI tractography

All participants were imaged with clinical 3T MRI scanners (MAGNETOM Skyra, Siemens Medical Systems, Erlangen, Germany) at Boston Children's Hospital. DICOM files of diffusion-weighted MRI were accessed through the Children's Research and Integration System (Pienaar et al., 2015). Thirty diffusion-weighted measurements ($b = 1000$ s/mm^2) and one to ten non-diffusion weighted measurements ($b = 0$ s/mm^2) were acquired (repetition time [TR] 4300–12929 ms; echo time [TE] 88–94 ms; voxel size 1.72 × 1.72 × 2.0 mm; matrix size 128 × 128; flip angle 90 degrees with a head coil). Images with motion artifacts were excluded based on visual assessment (motion correction software was not used). Eighteen diffusion MR images were obtained from 18 participants with SNHL aged

Author Manuscript Author Manuscript Author Manuscript Author Manuscript

under 10 YO. High angular resolution diffusion imaging (HARDI) (Tuch et al., 2002) was used to reconstruct fibers with Diffusion Toolkit (http;//trackvis.org), using the fiber assignment by continuous tracking (FACT) algorithm (Mori et al., 1999). We did not use an FA threshold to terminate tractography (e.g. Takahashi et al., 2012), but instead used a brain mask to perform tractography within the brain. Callosal pathways (CP) and 6 associational cortico-cortical fibers (arcuate fasciculus [AF], inferior longitudinal fasciculus [ILF], inferior fronto-occipital fasciculus [IFOF], uncinate fasciculus [UF], cingulum fasciculus [CF], and fornix [Fx]) in both hemispheres were identified and visualized using TrackVis (http;//trackvis.org), as in previous analyses (Takahashi et al., 2012; Xu et al., 2014; Cohen et al., 2016; Shiohama et al., 2019b, 2020).

Anatomic and tractography atlases (Catani & Thiebaut de Schotten, 2008; Mori & Tournier, 2013; Thiebaut de Schotten et al., 2011) were used to guide regions of interest (ROI) placements on non-diffusion-weighted (b0) images and color FA maps in order to delineate the fibers of interest. Two neuroscientists (T.S. and E.T.) identified all tracts through manual ROI placement and assessed resulting courses of fibers in the same way as explained in our past publications (e.g. Cohen et al., 2016; Re et al., 2016). For the AF, CF and Fx fibers, several ROIs were placed along the white matter regions for each fiber shown in the atlases. For the CP, an ROI was drawn in the corpus callosum in a median sagittal plane. For the ILF, IFOF, and UF fibers, two sphere ROIs were used for each region in their pathways: anterior temporal and occipital regions for the ILF, inferior frontal and occipital regions for the IFOF, and inferior frontal and anterior temporal regions for the UF. These ROIs were used as starting and stopping ROIs. When we did not identify any fibers between the starting/stopping ROIs, the distance between the two ROIs were gradually reduced until we found a part of the fibers. Excess erroneous fibers due to the large size of the ROIs were manually excluded using additional sphere ROIs. The size of all ROIs were carefully optimized to exclude other white matter fibers by changing the size and location several times. The color-coding of fibers will be based on a standard red-green-blue (RGB) code, applied to the vector between the endpoints of each fiber (red for right-left, blue for dorsal-ventral, and green for anterior-posterior). The volume, length, FA and apparent diffusion coefficient (ADC) of each identified pathway were calculated and compared with NC participants.

2.3. Statistical analysis

Each fiber pathway measurement in SNHL and NC participants, a univariate General Linear model ($p<0.05$) were constructed to evaluate the effects of binary or continuous covariates (age and gender). Using statistical function in Excel (Microsoft Corporation, WA) formula, critical values from the F-distribution calculation were determined to be F.INV.RT (0.05,4,29) = 2.70 and F.INV.RT (0.05,1,29) = 4.18 for the corrected model and each covariate, respectively. Cohen's $d = 0.8$ was recognized as a large effect size (Cohen, 1992). IBM SPSS Statistics version 19 (IBM Corp. Armonk, NY) was used for the statistical analysis.

Author Manuscript Author Manuscript Author Manuscript Author Manuscript

3. Results

3.1. Patient characteristics

We collected 17 MRI datasets from 17 participants with SNHL and compared them to those of NC after excluding one MRI dataset with poor quality that could not been processed through the software used (see **Experimental Procedures**). Gender and age at MRI scans in SNHL participants were matched to those of NC (ratio of males, SNHL 11/17, NC 11/17; age at scans, SNHL mean 3.8 YO [standard deviation 2.2], NC 3.7 [2.4], [T (32) = 0.0073, p = 0.994]) (Table 1).

3.2. HARDI tractography

We identified the AF, UF, CF, Fx, CP, ILF, and IFOF in SNHL and NC participants using HARDI tractography (Figure 1). Among the 17 participants with SNHL, the left ILF and left IFOF in participant (2.9 YO boy), right ILF in participant (3.3 YO boy), and right IFOF in three participants (2.9 YO boy, 3.3 YO boy, and 3.2 YO girl) were partly undetected. Therefore, the measurements of the ILF and IFOF were statistically compared between only 14 participants in each group who had full lengths of the ILF and IFOF detected (Table 1).

The ratio of volumes, length, FA, and ADC values in SNHL to NC ranged 0.43 – 0.86, 0.75 – 1.66, 0.89 – 1.07, and 1.14 – 1.36, respectively (Table 2, 3).

The presence of SNHL was an independent significant factor in the decreased volumes of the bilateral UF, Fx, ILF, and IFOF, the increased length of the bilateral UF, ILF, and IFOF, and left Fx, the decreased length of the bilateral CF, and increased ADC values in the bilateral AF, UF, CF, Fx, ILF, and IFOF, and CP. FA value showed no statistically significant differences (Table 4,5).

4. Discussion

We focused on long association fibers in SNHL using diffusion MRI tractography metrics and, in multiple fibers, found decreased volumes, increased lengths, and higher ADC values without difference of FA values in SNHL compared to NC.

4.1. HARDI tractography

In this study, we utilized HARDI instead of traditional diffusion tensor imaging (DTI), due to HARDI's potential advantage for detecting fibers in immature brains, which posse a surplus of unmyelinated or hardly myelinated fibers (e.g. Takahashi et al., 2014; Wilkinson et al., 2017; Frank, 2002). HARDI theoretically enables better differentiation within a voxel by utilizing information about water diffusivity from many more directions than DTI (Tuch et al., 2003). The white matter fibers in SNHL have been analyzed in only a few studies using tract-based spatial statistics (TBSS), which showed lower FA values of the bilateral AF, UF, ILF, and IFOF in profound SNHL patients aged below 4 years (Wang S et al., 2019; Park et al., 2018). In contrast, other measurements (volume, lengths, and ADC values) of long association fibers in SNHL have not been focused on so far. In our study, lower volumes of the bilateral UF, Fx, ILF, and IFOF were observed in children with SNHL. Interestingly, the ILF and IFOF were undetected in three participants with profound SNHL.

Author Manuscript Author Manuscript Author Manuscript Author Manuscript

Although recognizable brain atrophy was not observed in participants in this study, the possibility that these regional changes are affected by partial volume effects, such as gray matter of CSF contamination (Roine et al., 2014) or multiple fiber configurations (Jeurissen et al., 2013; Vos et al., 2011) cannot be completely excluded.

4.2. Long association fibers and cognitive functions

The long association fibers are involved in language processing (Hickok & Peeppoel, 2007; Friederici et al., 2015) and other cognitive functions. The AF is a lateral associative bundle, which is directly and indirectly connecting Broca's area (in the inferior frontal cortex), Geschwind's area (in the inferior parietal cortex), and Wernicke's area (in the superior temporal cortex) (Friedrici, 2015; Catani et al., 2005). The right AF also participates in visuospatial processing (Doricchi et al., 2008), prosody, and semantic processing (Catani et al., 2007). The UF possibly plays a role in emotion processing (Gaffan and Wilson, 2008; Ross, 2008), memory (Gaffan and Wilson, 2008; Ross, 2008), and language function (Catani and Mesulam, 2008). The CF and Fx are part of the limbic system (Catani et al., 2002; Catani & Thiebaut de Schotten, 2008), related to attention, memory, and emotions (Gaffan and Wilson, 2008; Ross, 2008; Rudrauff et al. 2008). The ILF and IFOF, which mainly connect regions of the fronto-parieto-temporal network, can be considered as a part of the speech processing stream (dual stream model) (Hickok and Poeppel, 2007). The ILF is a ventral associative bundle connecting the occipital and ipsilateral temporal lobes (Catani et al., 2002; Catani & Thiebaut de Schotten, 2008), which potentially governs face recognition (Fox et al., 2008), visual perception (Ffytche, 2008), reading (Epelbaum et al., 2008), and visual memory (Ross, 2008). The IFOF is a ventral associative bundle connecting the ventral occipital lobe and the orbitofrontal cortex (Catani et al., 2002; Catani & Thiebaut de Schotten, 2008), which is potentially linked to reading (Catani & Mesulam, 2008), attention (Doricchi et al., 2008), and visual processing (Fox et al., 2008; Rudrauff et al., 2008).

4.3. FA and ADC values on HARDI-derived fibers

The FA and ADC values represent the degree of directionality of microstructures and the degree of water diffusivity, respectively. The pattern of increased ADC values with decreased FA values in cerebral white matter has been associated with vasogenic edema (Pasternak et al., 2009), multiple sclerosis (Vishwas et al., 2013; Roosendaal et al., 2009), and the infantile period (Löbel et al., 2009). The pattern of decreased volume and increased ADC values with normal FA values, which was observed in long association fibers in the SNHL group in this study, may indicate the presence of a low density of cortico-cortical fibers in SNHL, although histopathological observation could not be carried out by our study or other investigators.

4.4. Impairment of the long association fibers and auditory deprivation

It remains unclear whether these changes in long association fibers in participants with SNHL was purely caused by auditory deprivation during intrauterine and early infantile period. Because we did not assess fetal brain MRI of both groups before the establishment of auditory systems, there is the possibility that another factor such as cerebral hypoxia led to both SNHL and affected long association fibers. However, we excluded patients with congenital disorders, perinatal brain damage, and premature birth by physical examination

Author Manuscript Author Manuscript Author Manuscript Author Manuscript

and MRI qualitative study. Even mild to moderate types of peripheral hypoxic ischemia encephalopathy present subsequent cerebral volume loss (Bregnant et al., 2013; Bano et al., 2017), and our SNHL participants showed no significant cerebral volume loss (see our previous report, Shiohama et al., 2019a), suggesting that the SNHL participants in our study had no profound perinatal brain damages.

Our previous study of CHARGE syndrome showed decreased volumes, increased lengths, and increased ADC without difference of FA values in multiple long association fibers, as compared to NC (Shiohama et al., 2019b). Interestingly, although patients with CHARGE syndrome were clinically excluded from participants in the current study, the pattern of measurements for HARDI-derived long association fibers in SNHL was similar to those in CHARGE syndrome (Shiohama et al., 2019b). Since hearing loss due to cranial nerve aphasia and / or semicircular canal hypoplasia is often observed in patients with CHARGE syndrome (Hoch et al., 2017), the differences between CHARGE syndrome and NC groups may partly depend on the presence of SNHL in CHARGE syndrome.

4.5. Limitations

Some limitations exist in this study. First, the possible presence of selection bias (healthcare access bias) could not be excluded because this study was retrospectively carried out in a single medical facility. Second, although we excluded patients with congenital disorders, perinatal brain damage, and premature birth to exclude major confounders, our medical records did not include the information regarding the developmental quotient, cognitive function except for auditory function, and handedness. Future studies are necessary to test associations between these factors and affected HARDI-derived fibers in SNHL. Third, MRI acquisition was carried out using clinical scans across many years, therefore: diffusion parameters in our study sometimes varied, although routine clinical scans usually use pre-set parameters to quickly diagnose. Lastly, the proportion of degree of hearing loss in this study (M-M 71%, M-P 29%) did not completely meet the proportions in a previous cross-section study (M-M 57%, M-P 43%) (Yoshinaga-Itano et al., 2017), and studies using TBSS (profound 100%) (Wang S et al., 2019; Wang H et al., 2019; Park et al., 2018). The difference of enrollment criteria potentially affects universality of analysis results. Another limitation is that we could not account intracerebral volume as covariates, because our data set did not include t1-weighted images of the neurotypical controls. Therefore, we could not completely exclude the possibility of whole brain volume to affect the measurements of the long association fibers.

5. Conclusion

Our quantitative study of HARDI-derived long association fibers in participants with SHNL showed increased length, decreased volume, and higher ADC in multiple fibers, compared to those of NC. The impairment of long association fibers in SNHL may partly be related to the association of cognitive dysfunction with SNHL.

Author Manuscript Author Manuscript Author Manuscript Author Manuscript

Acknowledgments

We thank Elizabeth Ethier for proofreading this paper. This research project was supported by National Institutes of Health (R01HD078561, R21MH118739, R21HD098606, and R03NS101372) to E.T., Natural Science and Engineering Research Council of Canada's Canada Research Chair grant (231266), a Canada Foundation for Innovation and Nova Scotia Research and Innovation Trust infrastructure grant (R0176004), and a St. Francis Xavier University research startup grant (R0168020) to J.L.

Abbreviations

ADC	apparent diffusion coefficient
AF	arcuate fasciculus
CC	corpus callosum
CF	cingulum fasciculus
CP	callosal pathways
DTI	diffusion tensor imaging
FA	fractional anisotropy
Fx	Fornix
HARDI	high-angular resolution diffusion imaging
IFOF	inferior fronto-occipital fasciculus
ILF	inferior longitudinal fasciculus
MRI	magnetic resonance imaging
NC	neurotypical controls
SNHL	sensorineural hearing loss
TBSS	tract-based spatial statistics
UF	uncinate fasciculus
YO	years old

Reference

Bano S, Chaudhary V, Garga UC (2017). Neonatal Hypoxic-ischemic Encephalopathy: A Radiological Review. J Pediatr Neurosci,12,1–6. [PubMed: 28553370]

Berger C, Kühne D, Scheper V, Kral A (2017). Congenital deafness affects deep layers in primary and secondary auditory cortex. J Comp Neurol,525,3110–3125. [PubMed: 28643417]

Bergeson TR, Houston DM, Miyamoto RT (2010). Effects of congenital hearing loss and cochlear implantation on audiovisual speech perception in infants and children. Restor Neurol Neurosci,28,157–165. [PubMed: 20404405]

Bregant T, Rados M, Vasung L, et al. (2013). Region-specific reduction in brain volume in young adults with perinatal hypoxic-ischaemic encephalopathy. Eur J Paediatr Neurol,17,608–614. [PubMed: 23746926]

Author Manuscript Author Manuscript Author Manuscript Author Manuscript

Buckley KA, Tobey EA (2011). Cross-modal plasticity and speech perception in pre- and postlingually deaf cochlear implant users. Ear Hear,32,2–15. [PubMed: 20829699]

Catani M, Allin MP, Husain M, Pugliese L, Mesulam MM, Murray RM, Jones DK (2007). Symmetries in human brain language pathways correlate with verbal recall. Proc Natl Acad Sci U S A,104,17163–17168. [PubMed: 17939998]

Catani M, Howard RJ, Pajevic S, Jones DK (2002). Virtual in vivo interactive dissection of white matter fasciculi in the human brain. Neuroimage,171,77–94.

Catani M, Jones DK, ffytche DH (2005). Perisylvian language networks of the human brain. Ann Neurol,57,8–16. [PubMed: 15597383]

Catani M, Mesulam M (2008). The arcuate fasciculus and the disconnection theme in language and aphasia: history and current state. Cortex,44,953–961. [PubMed: 18614162]

Catani M, Thiebaut de Schotten M (2008). A diffusion tensor imaging tractography atlas for virtual in vivo dissections. Cortex,44,1105–1132. [PubMed: 18619589]

Chang Y, Lee HR, Paik JS, Lee KY, Lee SH (2012). Voxel-wise analysis of diffusion tensor imaging for clinical outcome of cochlear implantation: retrospective study. Clin Exp Otorhinolaryngol,5,S37–42. [PubMed: 22701772]

Cohen AH, Wang R, Wilkinson M, MacDonald P, Lim AR, Takahashi E (2016). Development of human white matter fiber pathways: From newborn to adult ages. Int J Dev Neurosci,50,26–38. [PubMed: 26948153]

Cohen J (1992). A power primer. Psychol Bull,112,155–159. [PubMed: 19565683]

Doricchi F, Thiebaut de Schotten M, Tomaiuolo F, Bartolomeo P (2008). White matter (dis)connections and gray matter (dys)functions in visual neglect: gaining insights into the brain networks of spatial awareness. Cortex,44,983–995. [PubMed: 18603235]

Dye MW, Hauser PC (2014). Sustained attention, selective attention and cognitive control in deaf and hearing children. Hear Res,309,94–102. [PubMed: 24355653]

Dye MW (2014). Temporal entrainment of visual attention in children: effects of age and deafness. Vision Res,105,29–36. [PubMed: 25236173]

Epelbaum S, Pinel P, Gaillard R, Delmaire C, Perrin M, Dupont S, Dehaene S, Cohen L (2008). Pure alexia as a disconnection syndrome: new diffusion imaging evidence for an old concept. Cortex,44,962–974. [PubMed: 18586235]

Ffytche DH (2008). The hodology of hallucinations. Cortex,44,1067–1083. [PubMed: 18586234]

Filley CM, Fields RD(2016). White matter and cognition: making the connection. J Neurophysiol,116:2093–2104. [PubMed: 27512019]

Fox CJ, Iaria G, Barton JJ (2008). Disconnection in prosopagnosia and face processing. Cortex,44,996–1009. [PubMed: 18597749]

Frank LR (2002). Characterization of anisotropy in high angular resolution diffusion-weighted MRI. Magn Reson Med,47:1083–1099. [PubMed: 12111955]

Friederici AD (2015). White-matter pathways for speech and language processing. Handb Clin Neurol,129,177–186. [PubMed: 25726269]

Gaffan D, Wilson CR (2008). Medial temporal and prefrontal function: recent behavioural disconnection studies in the macaque monkey. Cortex, 44,928–935. [PubMed: 18585697]

Garel C, Chantrel E, Elmaleh M, Brisse H, Sebag G (2003). Fetal MRI: normal gestational landmarks for cerebral biometry, gyration and myelination. Childs Nerv Syst,19,422–425. [PubMed: 12879340]

Hickok G, Poeppel D (2007). The cortical organization of speech processing. Nat Rev Neurosci,8,393–402. [PubMed: 17431404]

Hoch MJ, Patel SH, Jethanamest D, et al. (2017). Head and neck MRI findings in CHARGE syndrome. AJNR Am. J. Neuroradiol,38,2357–2363. [PubMed: 28705814]

Hribar M, Suput D, Carvalho AA, Battelino S, Vovk A (2014). Structural alterations of brain grey and white matter in early deaf adults. Hear Res,318,1–10. [PubMed: 25262621]

Jeurissen B, Leemans A, Tournier JD, Jones DK, Sijbers J (2013). Investigating the prevalence of complex fiber configurations in white matter tissue with diffusion magnetic resonance imaging. Hum Brain Mapp,34:2747–2766. [PubMed: 22611035]

Author Manuscript Author Manuscript Author Manuscript Author Manuscript

Jiang M, Wen Z, Long L, et al. (2019). Assessing Cerebral White Matter Microstructure in Children With Congenital Sensorineural Hearing Loss: A Tract-Based Spatial Statistics Study. Front Neurosci,13,597. [PubMed: 31293368]

Kral A, Kronenberger WG, Pisoni DB, O'Donoghue GM (2016). Neurocognitive factors in sensory restoration of early deafness: a connectome model. Lancet Neurol,15,610–621. [PubMed: 26976647]

Kral A, O'Donoghue GM (2010). Profound deafness in childhood. N Engl J Med,363,1438–1450. [PubMed: 20925546]

Kral A (2013). Auditory critical periods: a review from system's perspective. Neuroscience,247,117–133. [PubMed: 23707979]

Kronenberger WG, Beer J, Castellanos I, Pisoni DB, Miyamoto RT (2014). Neurocognitive risk in children with cochlear implants. JAMA Otolaryngol Head Neck Surg,140,608–615. [PubMed: 24854882]

Levman J, MacDonald P, Lim AR, Forgeron C, Takahashi E (2017). A pediatric structural MRI analysis of healthy brain development from newborns to young adults. Hum Brain Mapp,38,5931–5942. [PubMed: 28898497]

Li J, Li W, Xian J, et al. (2012). Cortical thickness analysis and optimized voxel-based morphometry in children and adolescents with prelingually profound sensorineural hearing loss. Brain Res,1430,35–42. [PubMed: 22079323]

Löbel U, Sedlacik J, Güllmar D, Kaiser WA, Reichenbach JR, Mentzel HJ (2009). Diffusion tensor imaging: the normal evolution of ADC, RA, FA, and eigenvalues studied in multiple anatomical regions of the brain. Neuroradiology,51,253–263. [PubMed: 19132355]

Lomber SG, Meredith MA, Kral A (2010). Cross-modal plasticity in specific auditory cortices underlies visual compensations in the deaf. Nat Neurosci,13,1421–1427. [PubMed: 20935644]

Martines F, Martines E, Mucia M, Sciacca V, Salvago P (2013). Prelingual sensorineural hearing loss and infants at risk: Western Sicily report. Int J Pediatr Otorhinolaryngol,77,513–518. [PubMed: 23332734]

McCaskey U, von Aster M, O'Gorman R, Kucian K (2020). Persistent Differences in Brain Structure in Developmental Dyscalculia: A Longitudinal Morphometry Study. Front Hum Neurosci,14:272. [PubMed: 32765241]

Mori S, Crain BJ, Chacko VP, et al. (1999). Three-dimensional tracking of axonal projections in the brain by magnetic resonance imaging. Ann Neurol,45,265–269. [PubMed: 9989633]

Mori S, Tournier JD. Introduction to Diffusion Tensor Imaging. 1st. Academic Press; California: 2013, p.140

Oostra KM, Van Bladel A, Vanhoonacker AC, Vingerhoets G (2016). Damage to Fronto-Parietal Networks Impairs Motor Imagery Ability after Stroke: A Voxel-Based Lesion Symptom Mapping Study. Front Behav Neurosci,10:5. [PubMed: 26869894]

Park KH, Chung WH, Kwon H, Lee JM (2018). Evaluation of cerebral white matter in prelingually deaf children using diffusion tensor imaging. Biomed Res Int,2018,6795397. [PubMed: 29511689]

Pasternak O, Sochen N, Gur Y, Intrator N, Assaf Y (2009). Free water elimination and mapping from diffusion MRI. Magn Reson Med,62,717–730. [PubMed: 19623619]

Petro LS, Paton AT, Muckli L (2017). Contextual modulation of primary visual cortex by auditory signals. Philos Trans R Soc Lond B Biol Sci,372,20160104. [PubMed: 28044015]

Pienaar R, Rannou N, Bernal J, Hahn D, Grant PE (2015). ChRIS--A web-based neuroimaging and informatics system for collecting, organizing, processing, visualizing and sharing of medical data. Conf Proc IEEE Eng Med Biol Soc,2015,206–209.

Raij T, Ahveninen J, Lin FH, et al. (2010). Onset timing of cross-sensory activations and multisensory interactions in auditory and visual sensory cortices. Eur J Neurosci,31,1772–1782. [PubMed: 20584181]

Re TJ, Levman J, Lim AR, Righini A, Grant PE, Takahashi E (2016). High-angular resolution diffusion imaging tractography of cerebellar pathways from newborns to young adults. Brain Behav,7,e00589. [PubMed: 28127511]

Roine T, Jeurissen B, Perrone D, et al. (2014). Isotropic non-white matter partial volume effects in constrained spherical deconvolution. Front Neuroinform,2014;8:28.

Author Manuscript Author Manuscript Author Manuscript Author Manuscript

Roosendaal SD, Geurts JJ, Vrenken H, et al. (2009). Regional DTI differences in multiple sclerosis patients. Neuroimage,44,1397–1403. [PubMed: 19027076]

Ross ED (2008). Sensory-specific amnesia and hypoemotionality in humans and monkeys: gateway for developing a hodology of memory. Cortex,44,1010–1022. [PubMed: 18585698]

Rudrauf D, David O, Lachaux JP, et al. (2008). Rapid interactions between the ventral visual stream and emotion-related structures rely on a two-pathway architecture. J Neurosci,28,2793–2803. [PubMed: 18337409]

Sadato N, Okada T, Honda M, et al. (2005). Cross-modal integration and plastic changes revealed by lip movement, random-dot motion and sign languages in the hearing and deaf. Cereb Cortex,15,1113–1122. [PubMed: 15563723]

Shibata DK (2007). Differences in brain structure in deaf persons on MR imaging studied with voxel-based morphometry. AJNR Am J Neuroradiol,28,243–249. [PubMed: 17296987]

Shiohama T, Levman J, Vasung L, Takahashi E (2020). Brain morphological analysis in PTEN hamartoma tumor syndrome. Am J Med Genet A,182,1117–1129. [PubMed: 32162846]

Shiohama T, McDavid J, Levman J, Takahashi E (2019a). The left lateral occipital cortex exhibits decreased thickness in children with sensorineural hearing loss. Int J Dev Neurosci,76,34–40. [PubMed: 31173823]

Shiohama T, McDavid J, Levman J, Takahashi E (2019b). Quantitative brain morphological analysis in CHARGE syndrome. Neuroimage Clin,23,101866. [PubMed: 31154243]

Takahashi E, Folkerth RD, Galaburda AM, Grant PE (2012). Emerging cerebral connectivity in the human fetal brain: an MR tractography study. Cereb Cortex,22,455–464. [PubMed: 21670100]

Takahashi E, Hayashi E, Schmahmann JD, Grant PE (2014). Development of cerebellar connectivity in human fetal brains revealed by high angular resolution diffusion tractography. Neuroimage,96,326–333. [PubMed: 24650603]

Thiebaut de Schotten M, Ffytche DH, et al. (2011). Atlasing location, asymmetry and inter-subject variability of white matter tracts in the human brain with MR diffusion tractography. Neuroimage,54,49–59. [PubMed: 20682348]

Tomblin JB, Walker EA, McCreery RW, Arenas RM, Harrison M, Moeller MP (2015). Outcomes of Children with Hearing Loss: Data Collection and Methods. Ear Hear,36 Suppl 1,14S–23S. [PubMed: 26731154]

Tuch DS, Reese TG, Wiegell MR, Makris N, Belliveau JW, Wedeen VJ (2002). High angular resolution diffusion imaging reveals intravoxel white matter fiber heterogeneity. Magn Reson Med,48,577–582. [PubMed: 12353272]

Turgeon C, Champoux F, Lepore F, Ellemberg D (2012). Reduced visual discrimination in cochlear implant users. Neuroreport,23,385–389. [PubMed: 22415604]

Vetter P, Smith FW, Muckli L (2014). Decoding sound and imagery content in early visual cortex. Curr Biol,24,1256–1262. [PubMed: 24856208]

Vishwas MS, Healy BC, Pienaar R, Gorman MP, Grant PE, Chitnis T (2013). Diffusion tensor analysis of pediatric multiple sclerosis and clinically isolated syndromes. AJNR Am J Neuroradiol,34,417–423. [PubMed: 22859275]

Vos SB, Jones DK, Viergever MA, Leemans A (2011). Partial volume effect as a hidden covariate in DTI analyses. Neuroimage, 55:1566–1576. [PubMed: 21262366]

Wang H, Liang Y, Fan W, et al. (2019). DTI study on rehabilitation of the congenital deafness auditory pathway and speech center by cochlear implantation. Eur Arch Otorhinolaryngol,276,2411–2417. [PubMed: 31127414]

Wang S, Chen B, Yu Y, et al. (2019). Alterations of structural and functional connectivity in profound sensorineural hearing loss infants within an early sensitive period: A combined DTI and fMRI study. Dev Cogn Neurosci,38,100654. [PubMed: 31129460]

Watanabe H, Homae F, Nakano T, et al. (2013). Effect of auditory input on activations in infant diverse cortical regions during audiovisual processing. Hum Brain Mapp,34,543–565. [PubMed: 22102331]

Wilkinson M, Lim AR, Cohen AH, Galaburda AM, Takahashi E (2017). Detection and Growth Pattern of Arcuate Fasciculus from Newborn to Adult. Front Neurosci,11,389. [PubMed: 28769741]

Author Manuscript Author Manuscript Author Manuscript Author Manuscript

Wu C, Huang L, Tan H, et al. (2016). Diffusion tensor imaging and MR spectroscopy of microstructural alterations and metabolite concentration changes in the auditory neural pathway of pediatric congenital sensorineural hearing loss patients. Brain Res,1639,228–234. [PubMed: 25536303]

Xu G, Takahashi E, Folkerth RD, et al. (2014). Radial coherence of diffusion tractography in the cerebral white matter of the human fetus: neuroanatomic insights. Cereb Cortex,24,579–592. [PubMed: 23131806]

Yoshinaga-Itano C, Sedey AL, Wiggin M, Chung W (2017). Early Hearing Detection and Vocabulary of Children With Hearing Loss. Pediatrics,140,pii:e20162964. [PubMed: 28689189]

Author Manuscript Author Manuscript Author Manuscript Author Manuscript

Highlights

- Diffusion tractography-derived long association fibers were analyzed in deaf children
- Deaf children showed long hypovolemic fibers with high apparent diffusion coefficient value
- Impaired long association fibers may contribute to cognitive dysfunction in deaf children

Author Manuscript Author Manuscript Author Manuscript Author Manuscript

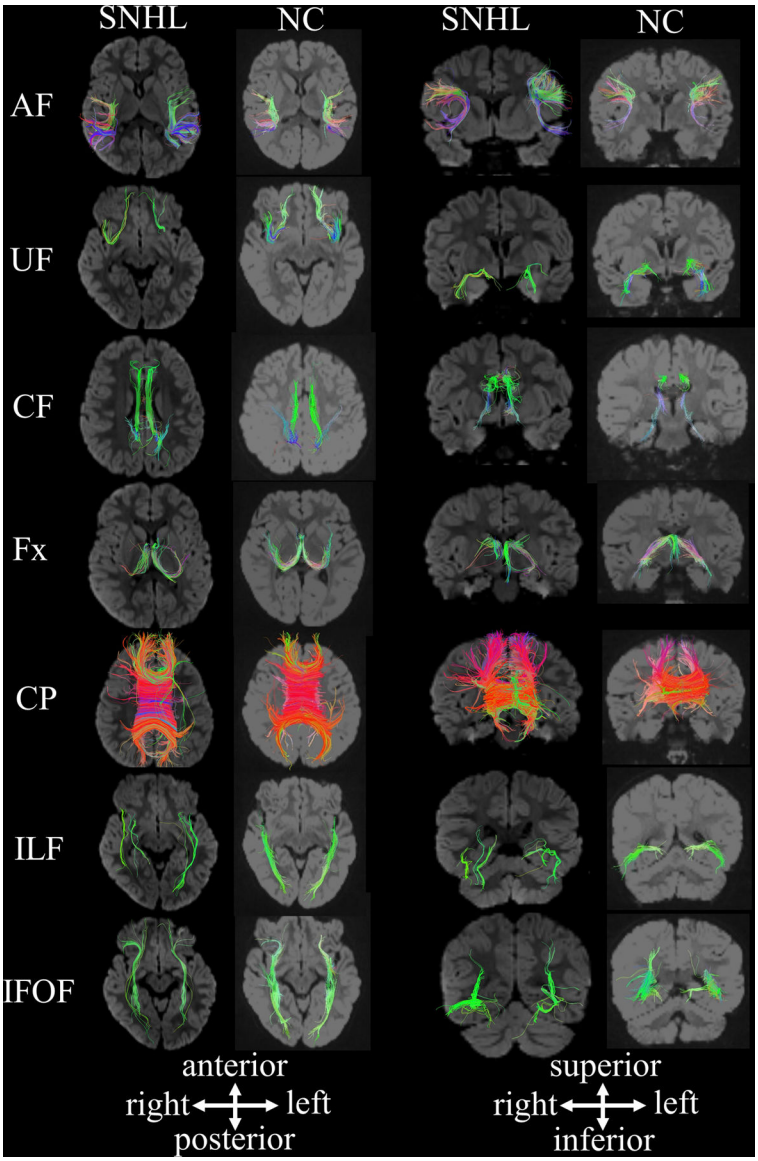

Figure 1.

Ventral and front views of high-angular resolution diffusion MR imaging tractography of a 2.2-year-old girl with sensorineural hearing loss (SNHL) and a 2.5-year-old neurotypical girl (NC). The density of uncinate fasciculus (UF), inferior longitudinal fasciculus (ILF), and inferior fronto-occipital fasciculus (IFOF) fibers in SNHL were visually lower compared to NC. Abbreviation: AF, arcuate fasciculus; CF, cingulum fasciculus; CP, callosal pathways; DTI, diffusion tensor imaging; Fx, fornix; IFOF, inferior fronto-occipital fasciculus; ILF, inferior longitudinal fasciculus; NC, neurotypical control; SNHL, sensorineural hearing loss; UF, uncinate fasciculus.

Author Manuscript

Author Manuscript

Author Manuscript

Author Manuscript

Table 1.

The background of SNHL and NC participants

HARDI tractography study (AF, UF, CF, Fx, and CP)	**SNHL (N = 17)**	**NC (N = 17)**
Male (N [%])	11/17 [65%]	11/17 [65%]
Age of years (mean [SD]) *a)*	3.8 [2.2]	3.7 [2.4]
in male *b)*	3.9 [2.5]	3.9 [2.4]
in female *c)*	3.5 [1.3]	3.5 [2.3]
Degree of SNHL (N [%])	M-M 12/17 [71%], M-P 5/17 [29%]	
HARDI tractography study (ILF and IFOF)	**SNHL (N = 14)**	**NC (N = 14)**
Male (N [%])	9/14 [64%]	9/14 [64%]
Age of years (mean [SD]) *d)*	3.9 [2.4]	3.8 [2.6]
in male *e)*	4.1 [2.8]	4.1 [2.6]
in female *f)*	3.6 [1.4]	3.2 [2.4]
Degree of SNHL (N [%])	M-M 12/14 [86%], M-P 2/14 [14%]	

The age of months showed no statistically significant difference between 2 groups.

a) $T(32)=0.0073$, $p = 0.994$;

b) $T(20)=0.016$, $p = 0.987$;

c) $T(8) = -0.014$, $p = 0.989$;

d) $T(26)= 0.125$, $p = 0.902$;

e) $T(16)=0$, $p = 1$;

f) $T(6) = 0.243$, $p = 0.816$.

Abbreviation; AF, arcuate fasciculus; CF, cingulum fasciculus; CP, callosal pathway; Fx, fornix; HARDI, High-angular resolution diffusion magnetic resonance imaging; IFOF, inferior fronto-occipital fasciculus; ILF, inferior longitudinal fasciculus; M-M, Mild to moderate; M-P, Moderately severe to profound; NC, Neurotypical control; SD, Standard deviation; SNHL, Sensorineural hearing loss; UF, uncinate fasciculus

Author Manuscript Author Manuscript Author Manuscript Author Manuscript

Table 2.

HARDI tractography (AF, UF, CF, Fx, and CP) of SNHL and NC participants

Measurements	SNHL (N=17) Mean [SD]	NC (N=17) Mean [SD]	The rate of SNHL/NC	Cohen's *d*
Volume (ml)				
AF, left	12.3 [4.6]	14.4 [5.2]	0.85	0.43
AF, right	11.4 [3.1]	15.2 [6.0]	0.75	0.79
UF, left	3.1 [1.5]	5.7 [0.9]	0.53	2.18
UF, right	2.8 [1.2]	5.9 [1.4]	0.48	2.38
CF, left	6.0 [1.4]	6.8 [1.8]	0.88	1.30
CF, right	5.5 [1.4]	6.3 [1.5]	0.87	1.13
Fx, left	4.0 [1.2]	6.2 [1.9]	0.65	1.38
Fx, right	4.0 [1.7]	6.0 [2.1]	0.68	1.02
CP	83.7 [21.4]	97.6 [37.6]	0.86	0.45
Lengths (mm)				
AF, left	47.8 [14.2]	43.9 [11.0]	1.09	0.31
AF, right	45.7 [12.6]	41.8 [8.2]	1.09	0.36
UF, left	54.5 [16.5]	39.0 [11.2]	1.40	1.10
UF, right	66.0 [18.0]	41.7 [11.6]	1.58	1.61
CF, left	29.8 [12.8]	39.8 [10.4]	0.75	0.03
CF, right	24.8 [8.6]	36.2 [7.8]	0.69	0.88
Fx, left	50.9 [17.2]	34.1 [7.5]	1.49	1.27
Fx, right	35.7 [14.6]	31.9 [8.3]	1.12	0.32
CP	69.7 [13.3]	63.8 [13.0]	1.09	0.46
FA				
AF, left	0.42 [0.05]	0.42 [0.07]	1.01	0.04
AF, right	0.42 [0.04]	0.42 [0.06]	0.99	0.05
UF, left	0.40 [0.05]	0.39 [0.07]	1.02	0.14
UF, right	0.40 [0.04]	0.39 [0.08]	1.02	0.15
CF, left	0.43 [0.07]	0.43 [0.07]	1.00	0.18
CF, right	0.41 [0.05]	0.42 [0.07]	0.98	0.22
Fx, left	0.36 [0.06]	0.38 [0.08]	0.96	0.22
Fx, right	0.33 [0.04]	0.37 [0.09]	0.89	0.59
CP	0.56 [0.03]	0.52 [0.07]	1.07	0.66
ADC ($mm^2/s \times 10^{-4}$)				
AF, left	8.9 [1.2]	7.5 [1.7]	1.19	0.95
AF, right	8.8 [0.6]	7.5 [1.7]	1.17	0.99
UF, left	9.1 [0.6]	7.9 [1.5]	1.15	1.02
UF, right	9.3 [0.5]	7.9 [1.5]	1.17	1.15
CF, left	9.2 [0.7]	7.7 [1.6]	1.18	1.18
CF, right	9.2 [0.6]	7.7 [1.5]	1.20	1.31

Author Manuscript

Author Manuscript

Author Manuscript

Author Manuscript

Measurements	SNHL (N=17) Mean [SD]	NC (N=17) Mean [SD]	The rate of SNHL/NC	Cohen's *d*
Fx, left	12.8 [1.7]	9.5 [2.1]	1.35	1.75
Fx, right	13.1 [2.1]	9.7 [2.3]	1.36	1.59
CP	9.5 [0.8]	7.69 [1.8]	1.23	1.27

Abbreviation; ADC, apparent diffusion coefficient; AF, arcuate fasciculus; CF, cingulum fasciculus; CP, callosal pathway; FA, fractional anisotropy; Fx, fornix; HARDI, High-angular resolution diffusion magnetic resonance imaging; NC, Neurotypical control; SD, Standard deviation; SNHL, Sensorineural hearing loss; UF, uncinate fasciculus

Author Manuscript Author Manuscript Author Manuscript Author Manuscript

Table 3.

HARDI tractography (ILF and IFOF) of SNHL and NC participants

Measurements	SNHL (N=14) Mean [SD]	NC (N=14) Mean [SD]	The rate of SNHL/NC	Cohen's *d*
Volume (ml)				
ILF, left	4.8 [2.3]	7.9 [1.6]	0.60	1.58
ILF, right	3.6 [1.2]	7.9 [1.8]	0.45	2.84
IFOF, left	5.7 [2.3]	12.2 [2.8]	0.47	2.55
IFOF, right	5.5 [2.0]	12.8 [3.4]	0.43	2.63
Lengths (mm)				
ILF, left	67.0 [10.8]	50.2 [6.3]	1.34	1.91
ILF, right	66.4 [14.5]	43.2 [6.1]	1.54	2.09
IFOF, left	98.2 [20.5]	59.1 [13.4]	1.66	2.26
IFOF, right	96.6 [23.3]	60.6 [9.4]	1.59	2.02
FA				
ILF, left	0.45 [0.06]	0.48 [0.07]	0.95	0.38
ILF, right	0.44 [0.06]	0.47 [0.07]	0.93	0.48
IFOF, left	0.48 [0.05]	0.48 [0.06]	0.99	0.09
IFOF, right	0.47 [0.04]	0.47 [0.06]	1.00	0.04
ADC ($mm^2/s \times 10^{-4}$)				
ILF, left	9.6 [0.9]	8.2 [1.8]	1.16	0.93
ILF, right	9.6 [0.9]	8.3 [1.9]	1.16	0.87
IFOF, left	9.2 [0.9]	8.0 [1.7]	1.15	0.89
IFOF, right	9.2 [0.8]	8.0 [1.7]	1.14	0.87

Abbreviation; ADC, apparent diffusion coefficient; FA, fractional anisotropy; HARDI, High-angular resolution diffusion magnetic resonance imaging; IFOF, inferior fronto-occipital fasciculus; ILF, inferior longitudinal fasciculus; NC, Neurotypical control; SD, Standard deviation; SNHL, Sensorineural hearing loss

Author Manuscript Author Manuscript Author Manuscript Author Manuscript

Table 4.

The Effects of Covariates on HARDI tractography Measurements (AF, UF, CF, Fx, and CP); Univariate General Linear Model

Measurements	Adjusted R^2	Corrected model	SNHL	Gender	Age
Volume					
AF, left	0.077	F=0.41, p=0.80	F=1.16, p=0.29	F=0.07, p=0.80	F=0.09, p=0.77
AF, right	0.080	F=1.72, p=0.17	F=3.55, p=0.07	F=0.06, p=0.82	F=0.71, p=0.40
UF, left	0.508	**F=9.52, p=4.8×10^{-5}**	**F=32.3, p=3.8×10^{-6}**	F=0.0016, p=0.97	F=0.29, p=0.59
UF, right	0.591	**F=12.9, p=3.7×10^{-6}**	**F=44.0, p=2.8×10^{-7}**	F=0.31, p=0.58	F=2.97, p=0.095
CF, left	0.016	F=0.87, p=0.49	F=2.7, p=0.11	F=0.15, p=0.70	F=0.64, p=0.43
CF, right	0.004	F=0.96, p=0.44	F=3.0, p=0.09	F=0.01, p=0.91	F=0.83, p=0.37
Fx, left	0.278	**F=4.2, p=8.6×10^{-3}**	**F=15.3, p=5.1×10^{-4}**	F=0.068, p=0.80	F=1.03, p=0.32
Fx, right	0.210	**F=3.2, p=0.027**	**F=9.0, p=5.5×10^{-3}**	F=2.8, p=0.11	F=0.61, p=0.44
CP	0.261	**F=3.9, p=0.011**	F=2.9, p=0.10	**F=4.5, p=0.043**	**F=9.1, p=5.3×10^{-3}**
Lengths					
AF, left	0.071	F=0.45, p=0.77	F=0.64, p=0.43	F=4.3×10^{-3}, p=0.95	F=1.03, p=0.32
AF, right	0.034	F=0.73, p=0.58	F=1.7, p=0.20	F=0.58, p=0.45	F=0.13, p=0.72
UF, left	0.199	**F=3.1, p=0.03**	**F=11.1, p=2.4×10^{-3}**	F=0.95, p=0.34	F=0.22, p=0.64
UF, right	0.366	**F=5.8, p=1.5×10^{-3}**	**F=19.2, p=1.4×10^{-4}**	F=1.16, p=0.29	F=0.77, p=0.39
CF, left	0.206	**F=3.1, p=0.029**	**F=6.2, p=0.019**	F=0.70, p=0.41	**F=5.3, p=0.03**
CF, right	0.310	**F=4.7, p=4.8×10^{-3}**	**F=13.7, p=8.8×10^{-4}**	F=2.7×10^{-3}, p=0.96	F=1.9, p=0.18
Fx, left	0.278	**F=4.2, p=8.6×10^{-3}**	**F=9.5, p=4.5×10^{-3}**	F=0.51, p=0.48	F=0.14, p=0.71
Fx, right	0.016	F=0.87, p=0.49	F=0.38, p=0.54	F=0.18, p=0.67	F=1.72, p=0.20
CP	0.158	F=2.6, p=0.06	F=2.8, p=0.10	F=2.1, p=0.15	**F=5.2, p=0.03**
FA					
AF, left	0.061	F=1.5, p=0.22	F=0.02, p=0.88	F=1.9, p=0.18	F=3.8, p=0.06
AF, right	0.000	F=1.0, p=0.42	F=0.14, p=0.71	F=1.2, p=0.28	F=2.3, p=0.14
UF, left	0.076	F=0.42, p=0.79	F=0.2, p=0.66	F=1.1, p=0.29	F=0.24, p=0.63
UF, right	0.067	F=0.48, p=0.75	F=0.1, p=0.75	F=1.5, p=0.24	F=0.15, p=0.70
CF, left	0.082	F=0.38, p=0.82	F=0.01, p=0.92	F=0.17, p=0.68	F=1.3, p=0.26
CF, right	0.094	F=0.29, p=0.88	F=0.31, p=0.58	F=0.34, p=0.57	F=0.46, p=0.50
Fx, left	0.120	F=0.11, p=0.98	F=0.34, p=0.56	F=2.5×10^{-3}, p=0.96	F=0.09, p=0.77
Fx, right	0.026	F=0.79, p=0.54	F=2.4, p=0.13	F=0.18, p=0.67	F=0.26, p=0.62
CP	0.020	F=1.2, p=0.35	F=2.8, p=0.10	F=0.30, p=0.59	F=0.84, p=0.37
ADC					
AF, left	0.270	**F=4.1, p=0.01**	**F=9.0, p=5.4×10^{-3}**	F=3.6, p=0.068	F=4.0, p=0.054
AF, right	0.279	**F=4.2, p=8.4×10^{-3}**	**F=10.2, p=3.4×10^{-3}**	F=2.8, p=0.11	**F=4.3, p=0.046**
UF, left	0.256	**F=3.8, p=0.013**	**F=10.2, p=3.4×10^{-3}**	F=2.7, p=0.11	F=2.9, p=0.099
UF, right	0.284	**F=4.3, p=7.7×10^{-3}**	**F=12.8, p=1.3×10^{-3}**	F=2.2, p=0.15	F=2.5, p=0.12
CF, left	0.346	**F=5.4, p=2.3×10^{-3}**	**F=15.3, p=5.1×10^{-4}**	F=3.4, p=0.074	F=3.1, p=0.089

Author Manuscript

Author Manuscript

Author Manuscript

Author Manuscript

Measurements	Adjusted R^2	Corrected model	SNHL	Gender	Age
CF, right	0.353	**F=5.5, p=2.0×10^{-3}**	**F=16.9, p=2.9×10^{-4}**	F=2.4, p=0.13	F=3.0, p=0.093
Fx, left	0.406	**F=6.6, p=6.4×10^{-3}**	**F=21.1, p=7.8×10^{-5}**	F=0.22, p=0.65	F=1.05, p=0.31
Fx, right	0.423	**F=7.1, p=4.3×10^{-4}**	**F=17.1, p=2.8×10^{-4}**	F=2.8, p=0.103	F=0.025, p=0.87
CP	0.370	**F=5.8, p=1.4×10^{-3}**	**F=15.3, p=5.1×10^{-4}**	F=4.2, p=0.051	F=3.9, p=0.057

Bold numbers indicate values with a statistical significance. General Linear Model (P<0.05) was constructed to evaluate of binary or continuous covariates (gender and age). Statistically significant values from the F-distribution calculation were determined to be 2.70 and 4.18 for the corrected model and each covariate, respectively. Abbreviation; ADC, apparent diffusion coefficient; AF, arcuate fasciculus; CF, cingulum fasciculus; CP, callosal pathway; FA, fractional anisotropy; Fx, fornix; HARDI, High-angular resolution diffusion magnetic resonance imaging; SNHL, Sensorineural hearing loss; UF, uncinate fasciculus

Author Manuscript Author Manuscript Author Manuscript Author Manuscript

Table 5.

The Effects of Covariates on HARDI tractography Measurements (ILF and IFOF); Univariate General Linear Model

Measurements	Adjusted R^2	Corrected Model	SNHL	Gender	Age
Volume					
ILF, left	0.410	**F=5.7, p=2.5×10^{-3}**	**F=21.8, p=1.1×10^{-4}**	F=0.03, p=0.86	F=0.8, p=0.38
ILF, right	0.650	**F=13.5, p=8.3×10^{-6}**	**F=45.6, p=6.9×10^{-7}**	F=0.04, p=0.84	F=0.7, p=0.41
IFOF, left	0.619	**F=12.0, p=2.1×10^{-5}**	**F=45.2, p=7.5×10^{-7}**	F=0.09, p=0.76	F=1.8, p=0.20
IFOF, right	0.758	**F=22.1, p=1.3×10^{-7}**	**F=63.1, p=4.8×10^{-8}**	F=0.25, p=0.62	F=13.6, p=1.2×10^{-3}
Lengths					
ILF, left	0.466	**F=6.9, p=8.5×10^{-4}**	**F=24.4, p=5.4×10^{-5}**	F=1.7, p=0.20	F=0.3, p=0.57
ILF, right	0.473	**F=7.1, p=7.4×10^{-4}**	**F=26.2, p=3.5×10^{-5}**	F=0.51, p=0.48	F=0.05, p=0.82
IFOF, left	0.589	**F=10.7, p=4.9×10^{-5}**	**F=38.6, p=2.5×10^{-6}**	F=2.3, p=0.14	F=1.2, p=0.28
IFOF, right	0.646	**F=13.3, p=9.2×10^{-6}**	**F=42.4, p=1.2×10^{-6}**	**F=7.5, p=0.012**	F=3.7, p=0.068
FA					
ILF, left	0.105	F=1.8, p=0.16	F=1.6, p=0.22	F=0.42, p=0.53	**F=5.6, p=0.026**
ILF, right	0.059	F=1.4, p=0.26	F=2.6, p=0.12	F=0.01, p=0.93	F=2.7, p=0.11
IFOF, left	0.082	F=0.5, p=0.74	F=0.06, p=0.81	F=0.03, p=0.86	F=1.9, p=0.18
IFOF, right	0.033	F=0.8, p=0.55	F=0.01, p=0.91	F=0.79, p=0.38	F=2.7, p=0.12
ADC					
ILF, left	0.268	**F=3.5, p=0.023**	**F=8.3, p=8.6×10^{-3}**	F=2.9, p=0.104	F=3.9, p=0.062
ILF, right	0.285	**F=3.7, p=0.018**	**F=7.7, p=0.011**	F=3.2, p=0.08	**F=5.1, p=0.034**
IFOF, left	0.226	**F=3.0, p=0.041**	**F=6.7, p=0.016**	F=3.6, p=0.069	F=2.5, p=0.13
IFOF, right	0.261	**F=3.4, p=0.026**	**F=7.2, p=0.013**	F=3.2, p=0.089	**F=4.3, p=0.048**

Bold numbers indicate values with a statistical significance. General Linear Model (P<0.05) was constructed to evaluate of binary or continuous covariates (gender and age). Statistically significant values from the F-distribution calculation were determined to be 2.70 and 4.18 for the corrected model and each covariate, respectively. Abbreviation; ADC, apparent diffusion coefficient; FA, fractional anisotropy; HARDI, High-angular resolution diffusion magnetic resonance imaging; IFOF, inferior fronto-occipital fasciculus; ILF, inferior longitudinal fasciculus; SNHL, Sensorineural hearing loss